Available online at www.sciencedirect.com
ScienceDirect
Advances in Space Research 47 (2011) 563–574
ADVANCES IN SPACE RESEARCH (a COSPAR publication)
www.elsevier.com/locate/asr

Review

A review of instruments and methods for dosimetry in space

Jarvis A. Caffrey *, D.M. Hamby

Nuclear Engineering and Radiation Health Physics, 116 Radiation Center, Oregon State University, Corvallis, OR 97331, USA

Received 10 June 2010; received in revised form 30 September 2010; accepted 5 October 2010
Available online 30 October 2010

Abstract

Instruments and methods recently used for space radiation dosimetry are reviewed for the purposes of comparison and reference. Passive detection methods mentioned include track-etch, luminescent, nuclear emulsion, and metal foil detectors. These can provide a reliable source of data for all types of radiation, but often require processing that cannot occur in space. Experimental methods of LET determination using TLDs, such as the high temperature peak ratio (HTR) method, are also discussed. Portable readout passive detectors including Pille, MOSFET, and bubble detector systems provide a novel alternative to traditional passive detectors, but research is more limited and their widespread use has yet to be established. Active detectors including DOSTEL, CPDS, RRMD-III, TEPC, R-16, BBND, and the Liulin series are examined for technical details. These instruments allow the determination of dose in real-time, and some can determine LET of incident particles by measuring energy deposition over a known path-length, but size and power consumption limit their practical use for dosimetry. Improved neutron dosimetry and development of a small active or portable readout personnel dosimeter capable of accurate LET determination are important steps for managing the effects of long-term exposure to the space radiation environment.

Keywords: Space; Cosmic; Radiation; Dosimeters; Detectors

Contents

* Corresponding author.
E-mail addresses: jarvis.caffrey@gmail.com, caffreyj@onid.orst.edu (J.A. Caffrey).

0273-1177/$36.00 © 2010 COSPAR. Published by Elsevier Ltd. All rights reserved.
doi:10.1016/j.asr.2010.10.005

1. Introduction

Quantification of radiation dose to astronauts is difficult due to the complexity of the space radiation environment. Galactic cosmic rays (GCR) originating from cosmic events outside of the solar system contribute about half of the total effective dose received by astronauts in low-Earth orbit (LEO). The majority of the remaining dose is due to protons trapped within the Earth's magnetosphere. Secondary particles such as albedo neutrons reflecting from the Earth's atmosphere can also contribute a small dose, but this is often neglected. Perhaps most importantly, solar particle events (SPE) can deliver potentially lethal doses of radiation to astronauts traveling outside of the relative safety of Earth's magnetosphere, though these events are generally short-lived and comparatively rare (Benton and Benton, 2001). For astronauts within low-Earth orbit, these four sources all contribute to an immensely complex radiation field which varies as the spacecraft changes altitude and inclination, or passes through the South Atlantic Anomaly (SAA) where the inner proton belt intersects with the path of orbiting spacecraft. Secondary particles produced by scatter events within spacecraft increase complexity even further as the contents and orientation of the spacecraft changes.

Astronauts traveling in low-Earth orbit, such as onboard the space station, receive mean dose equivalents generally not exceeding 650 μSv/day (0.237 Sv/yr) (Benton and Benton, 2001). During deep space travel, astronauts will be subject only to galactic cosmic rays and rare solar particle events, but will receive much higher doses without the protection afforded by the Earth's magnetosphere. Little data is available for such an environment, but mean annual dose equivalents of around 0.5 Sv could be expected from GCR without contribution from SPE (Simonsen et al., 2000; Ballarini et al., 2006). Blood-forming-organ dose equivalent limits for astronauts within LEO are established by the NCRP Report No. 98 at 0.50 Sv/yr, with a sliding scale for total career dose dependent upon age and gender. The units for this limit were modified by NCRP Report No. 132, though the quantities remain essentially equivalent. The biological effects of GCR are still being studied and the NCRP requires more understanding before establishing dose limits for deep space travel.

While astronauts within low-Earth orbit are unlikely to exceed current dose limits, it is clear that future missions to the Moon and Mars may result in doses that approach or exceed recommendations. As such, the determination of dose requires instruments with great accuracy and sensitivity to the space radiation environment. In particular, it is critical to determine the linear energy transfer (LET) of incident radiation to make an accurate determination of equivalent dose. Simple measurements of absorbed dose do not account for the added biological harm of high LET radiation. Additional constraints include minimization of cost, weight, size, and power consumption due to the logistical challenges presented by space travel. Many instruments and techniques have been developed internationally by a variety of agencies, universities, and companies. This article provides a review of many of those devices, both passive and active, used in the determination of risk to astronauts from the space radiation environment.

2. Passive dosimetry

High-Z, high-energy (HZE) particles incident upon the hull and contents of spacecraft create a broad spectrum of secondary radiation that varies widely throughout the vessel. It is therefore necessary to quantify dose throughout the spacecraft and to each astronaut, rather than rely on single-point measurements. This requirement of widespread dosimetry lends itself to the use of passive detection methods that are small, economical, and can operate with no demands to the limited supply of electricity during space missions (see Tables 1 and 3).

Table 1
Comparison of passive detectors.

Dosimeter	Examples	Range of response	Type[a]	Absorbed vs. equivalent dose	Tissue equivalence
Plastic nuclear track detector	CR-39	5–10^3 keV/μm^{-1} (H_2O)	Hi, N	Equivalent dose	Yes
Luminescent detector	TLD-100, -600, -700, OSLD	<20 keV/μm^{-1} (tissue)	Lo, Hi, N	Absorbed dose: LET/Eq. dose unreliable in mixed fields	LiF: Yes Al_2O_3: No
Photographic emulsion	BR & Bya type NPE Film	0.2–10^3 keV/μm^{-1} (tissue)	Lo, Hi, N	Equivalent dose	No
Metal foil	Activation, fission No	–	Hi, N	Activation: Absorbed dose Foil + NTD: equivalent dose	
Portable readout TLD	"Pille" zystem	<20 keV/μm^{-1} (tissue)	Lo	Absorbed dose	No
MOSFET	EVARM	–	Lo	Absorbed dose	No
Bubble detector	MATROSHKA-R	Neutrons: 0.2–20 MeV	Hi, N	Equivalent dose	Yes

[a] Hi = high-LET charged particle; Lo = low LET (electron, gamma); N = neutron.

2.1. Track etch detectors

An effective method of dose determination from high linear energy transfer (LET) radiation is through the use of track etch detectors. Currently the most appropriate dosimeter for this application is the CR-39 plastic nuclear track detector (PNTD). CR-39 has a chemical composition of $C_{12}H_{18}O_7$ and is closest to tissue equivalence among track etch detectors (Zhou et al., 2008). As compared to other dosimetry methods, CR-39 provides the broadest range of response with good sensitivity to radiation with LET from 5 to 1000 keV μm^{-1}. It does not register dose contribution from low LET radiation, but this can be taken into account when used in conjunction with luminescent detectors.

High LET particles incident upon CR-39 weaken the plastic structure to create latent tracks as they traverse the material. During processing, the CR-39 is etched in a caustic solution (often sodium hydroxide), which dissolves the plastic at a constant rate. In locations where a particle has weakened the plastic, conical pits form on the detection surface. After a given time, the detector is removed from the solution and analyzed under a microscope. The number, size, and depth of pits in the material is determined, which, when combined with information regarding mass difference before and after etching, are used to determine an effective LET and dose to the plastic. Combining these values allows for determination of equivalent dose to astronauts contributed by high-LET radiation.

While computers are capable of performing automated analysis of the pitted plastic, it is more accurate and often faster to leave the analysis to an experienced researcher. The prevalence of material defects in the CR-39 leads to an abundance of pits which did not result from incident radiation, and automated scanning often fails to discriminate these from actual events (Zhou et al., 2008).

Standard CR-39 is sensitive to neutrons, though there is not an established method of discriminating those events from the charged particles which contribute a majority of the tracks. CR-39 can be used for neutron dosimetry, however, by sandwiching two PNTDs around a ^{6}LiF converter foil. One PNTD is covered in gadolinium or cadmium to discriminate thermal neutron contribution, while epithermal neutron dose is determined by measuring contribution from the ^{6}Li scatter reactions (Benton et al., 2001).

2.2. Luminescent detectors

Luminescent detectors (thermoluminescent detectors [TLDs] and optically stimulated luminescent detectors [OSLDs]) rely upon the ionization of a crystal to accumulate a measurement of dose which can be assessed at a later time. Ionization creates electron–hole pairs which migrate and store in trapping sites caused by dopant impurities in the crystal. When measured, the crystal is excited either by heating (TLD) or by stimulation from specific wavelengths of light (OSLD). As the lattice is excited, electrons and holes are freed from the traps and rejoin in recombination sites, again, caused by dopants in the crystal. This process of recombination releases visible light photons in a quantity that correlates with the dose accumulated during irradiation.

Optically stimulated luminescence is a comparatively new development and as such there is far less information published regarding its applications in space. Many of the principles of operation concerning TLD carry over to OSLD, though many improvements can be expected thanks to increased control of stimulation. For instance, rather than heating to release all electrons from their traps, a short pulse of light stimulation may release a small sample of electrons while retaining a majority of stored electrons. An OSL dosimeter can therefore be repeatedly analyzed without erasing its history to obtain consecutive doses in addition to an accumulated dose (Yukihara et al., 2006).

TLDs have proven remarkably effective in the assessment of dose in terrestrial applications and have been an important tool in space dosimetry for several decades. Unfortunately, TLDs suffer from two major problems when quantifying dose in space. First, TLDs respond with a decreased efficiency to high LET radiation caused by a saturation of electrons in the track of high LET particles. Though there are several competing processes at work, the details of which are beyond the scope of this article, this

saturation essentially fills up the crystal's trapping sites and prevents a fraction of the dose from being recorded (Horowitz et al., 2003). Secondly, traditional TLDs are ambiguous as to the quality of incident radiation, necessary information to determine an equivalent dose. Traditional TLDs have therefore systematically underreported dose received by astronauts. A few methods, detailed in the following sections, have been developed to counter these problems with varying degrees of success.

2.2.1. High temperature peak ratio

It was noted in 1972 by B. Jähnert (Bilski, 2010) that, during readout, the higher temperature peaks of the TLD glow curve show an increased relative response when exposed to high LET radiation. The ratio between the main peak and the high temperature peak may therefore be correlated to an effective LET value of the incident radiation to determine a quality factor and equivalent dose (Vana et al., 1996). This estimation of LET can also be used to correct for the TLD's decreased efficiency to densely ionizing radiation, deemed the HTR-B method (Berger et al., 2006).

It is important to note that the HTR method was shown to be unreliable in estimating quality factor during blind exposure tests, but can correct for efficiency with reasonable reliability using the HTR-B method (Bilski, 2010). Regardless, the HTR method provides an improvement of estimated dose over a traditional TLD, but is best suited to supplement data derived by other means. This process has seen many improvements in the past decade and was used as an additional estimator of equivalent dose in the MATROSHKA tissue equivalent phantom experiments (Berger et al., 2004) in spite of its questionable accuracy.

2.2.2. Multiple TLDs of varying efficiency

A more recently developed technique to determine incident LET involves the use of several TLD phosphors in unison (Bilski, 2006). Each crystal responds to high-LET radiation with varying efficiency while maintaining a more consistent efficiency to low LET radiation. In this manner, the dose from each crystal can be compared to provide an estimate of the dose contribution from high LET radiation. This method may provide some improvement of equivalent dose estimation, but is still under development and remains unreliable in mixed radiation fields (Bilski, 2006).

2.2.3. TLD & CR-39 packages

As previously mentioned (see Section 2.1), the CR-39 plastic nuclear track detector provides excellent response to high LET radiation, but is incapable of responding to sparsely ionizing radiation. Doses from both high LET and low LET radiation can be assessed separately, however, to create an accurate estimate of accumulated dose. By combining TLDs or OSLDs with PNTDs on a single personnel dosimeter, an accurate equivalent dose can be assessed across the entire LET spectrum. This is currently the most popular method of passive personnel dosimetry in space (Benton and Benton, 2001).

2.2.4. Luminescent neutron detection

TLDs are often used to estimate neutron dose in terrestrial applications and they can also be applied, with some degree of success, for estimation of neutron dose in space. TLDs made with LiF are well-suited for detecting slow neutrons by taking advantage of the $^{6}Li(n,\alpha)$ reaction to induce ionization within the crystal. This effect is enhanced in crystals enriched with ^{6}Li (TLD600) and suppressed in detectors made with ^{7}Li (TLD700). The comparison of these two detectors, irradiated simultaneously, can provide information about the presence of slow neutrons. The $^{6}Li(n,\alpha)$ cross-section decreases with increasing neutron energy, however, so this technique is less adept for detection of fast neutrons. It is possible to measure fast neutron contribution by encapsulating a standard TLD crystal, such as Al_2O_3, in polyethylene (Knoll, 2000).

2.3. Nuclear photographic emulsion

The use of photographic film was historically a preferred method of passive dosimetry. The need for development and processing, in addition to its sensitivity to light, moved preference toward other methods that are more stable and do not require counting of individual tracks. In space dosimetry, the relatively long duration of flight leads to darkening of the film by sparsely ionizing radiation and prevents accurate counting of heavy ion tracks.

Later developments in photographic emulsion have improved capability in space applications by increasing the LET threshold of detection within the emulsion to prevent excessive darkening. Tracks can be analyzed to measure the LET environment during exposure and, in so doing, the equivalent dose contribution from radiation with LET from 0.2 to 1000 keV μm^{-1} can be determined over the duration of a space mission (Akopova et al., 2005).

2.4. Metal foils

Foils can be used for measurement of neutron contribution, either through activation of a stable metal or through fission of a fissionable metal. Metals such as gold, tantalum, and cobalt are good candidates for activation by neutrons at varying energies (Badhwar et al., 2002). The low flux of neutrons and long duration of flight in which activation products decay away, however, cause poor statistics in the activation method (Benton et al., 2001).

More commonly used are foils of fissionable metal, sandwiched between layers of nuclear track detectors. Insensitive track detectors, such as mica, are preferred for this technique, as they can produce tracks from heavy fission fragments without interference from the high flux of charged particles. Metals such as ^{235}U, ^{238}U, ^{237}Np, and ^{209}Bi all fission with a high cross section for fast neutrons,

though radioactive properties preclude all but ^{209}Bi from use in space. ^{209}Bi also has a high fission cross section for energetic protons, however, so this technique requires additional information of the proton/neutron spectra to accurately determine equivalent dose (Benton et al., 2001).

2.5. Portable readout passive dosimetry

One of the most significant problems with passive dosimetry in space is the duration of exposure. A traditional luminescent detector or etched-track detector must be processed on Earth and will therefore accumulate a dose throughout the entire mission. A system which is capable of reading out a set of passive dosimeters onboard the spacecraft would prove to be valuable, especially if used in the context of a long-term mission such as a voyage to Mars.

2.5.1. Pille TLD system

The Hungarian "Pille" system (which translates to "butterfly" in English) was first developed for use on the Salyut-6 Space Station in 1980. Since then it has undergone several revisions, the latest of which is used on board the Russian segment of the International Space Station. This system utilizes a small readout machine that heats a set of 10 dosimeters and measures light output. Each dosimeter consists of a dysprosium-doped calcium sulfate crystal mounted to a resistive metal plate. The crystal and plate are sealed within a glass vacuum bulb, protected by a metal case. Metal contacts connect to the resistive metal plate which allow an electric current to heat the TLD crystal within the bulb (Apáthy et al., 2002).

The latest generations of the Pille system make use of microprocessors to automatically identify each dosimeter, provide timestamp information, and save the outputs to a removable flash card. In addition, a built-in thermometer and light source improve accuracy by accounting for ambient temperature and sensitivity changes in the photomultiplier tube. In usage on the ISS, one TLD is kept within the reader at all times with repeated readings every 90 min. Two dosimeters are used for extravehicular activities (EVAs) and the remaining seven dosimeters are placed throughout the Russian segment of the ISS for monthly readings of area dosimetry (Apáthy et al., 2007).

The Pille system suffers from the aforementioned problems of decreased high-LET efficiency and ambiguity regarding radiation quality (see Section 2.2). To account for this, LET data is supplemented by use of auxiliary dosimeters such as CR-39 PNTDs, LiF:Mg,Ti with the HTR method, or active LET spectrometers such as the Dosimetric Telescope (see Section 3.2.1) mentioned later in this article (Apáthy et al., 2002).

2.5.2. MOSFET

Metal oxide semiconductor field effect transistors are known to be useful in monitoring terrestrial gamma and X-ray fields, and have become popular for use in medical physics applications. The very small size of the detector allows for point measurements of dose during application of radiation for medical treatment and diagnostics, even within living subjects (Thomson and Nielsen, 1999).

MOSFET dosimeters consist of two electrodes embedded within a silicon substrate (see Fig. 1). A silicon oxide layer is implanted upon the silicon substrate in the gap between these electrodes, with a metal gate electrode fused to the top of the oxide layer. A current applied to the two outer electrodes, known as the source and drain electrodes, will not pass through the silicon substrate beneath the gate and oxide layers until an adequate negative voltage (deemed the threshold voltage) is applied to the metal gate electrode. This threshold voltage is subject to change as the dosimeter is irradiated. If ionization occurs within the oxide layer while a positive voltage is applied to the gate, electron/hole pairs are liberated. Electrons simply migrate into the metal electrode and are carried away by the positive voltage bias, while holes are drifted down into the interface of silicon oxide and silicon substrate. It is this increase in hole density within the substrate that increases the threshold voltage necessary to carry current between the source and drain electrodes, and this voltage difference can be correlated to dose with a high degree of accuracy.

MOSFET dosimeters have been used for many years in space applications, especially in the context of monitoring crew exposure during extra-vehicular activity. They have also been used for estimation of depth dose within the MATROSHKA phantom (Halill et al., 2010). Many advantages such as small size, permanent dose record, and an ability to work as either a passive or active dosimeter make the MOSFET a desirable option for monitoring the radiation environment. MOSFETs are most adept at measuring dose caused by photons and electrons, but are capable of measuring dose from protons as well (Kohno et al., 2006). They can also be used to estimate fast neutron dose by using a hydrogenous medium to produce recoil protons (Knoll, 2000). MOSFETS are not an ideal dosimeter, however, for reasons similar to that of luminescent detectors. Dose response for particles other than photons and electrons is dependent upon incident LET and energy, so accurate measurement of equivalent dose in a mixed radiation field is not currently possible with a simple MOSFET dosimeter alone. MOSFET has recently been used for

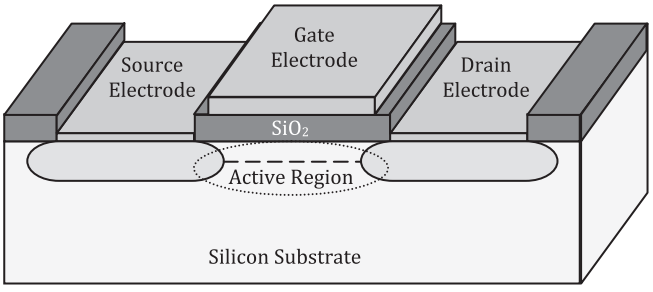

Fig. 1. Cross-section diagram of MOSFET detector. Adapted from Thomson and Nielsen (1999).

measurement of dose during proton therapy, but this application is made possible due to a monoenergetic beam with known LET distributions (Thomson and Nielsen, 1999). Regardless, the technology has potential for improvement and will continue to provide convenient and useful dosimetry on board the International Space Station.

2.5.3. Superheated bubble detector/mini reader

Bubble detectors present a novel approach to neutron detection in space. A volume of fluid is encapsulated within a container and subjected to a vacuum, causing the fluid to exist above its vaporization temperature without initiating vaporization. A molecular tension is therefore established, and the stored kinetic energy is capable of amplifying the effects of nuclear interactions as particles impart thermal energy to vaporize small amounts of fluid (Ing, 2001).

Bubble detectors were used as part of the MATROSHKA-R experiment, where small vials of superheated fluid were deposited within a spherical tissue equivalent phantom for measurement of neutron depth-dose. Each detector contained 10 ml of fluid, which was specially formulated to respond slowly and allow longer time periods between recompression and measurement. A small readout machine was included in the experiment for this purpose, which automatically scanned each detector vial to count the bubbles that formed before recompressing and resetting the vial. Calibrations are performed in relation to dose equivalent, so response is measured directly as such (Machrafi et al., 2009).

Bubble detectors respond well to neutrons, though their sensitivity to heavy charged particles complicates measurements. They can only be used for relatively short periods of time, as there are a limited number of bubbles capable of being read within the detector volume (Benton et al., 2001). Use of bubble detectors in space has so far been limited, though future missions plan to utilize a bubble-detector spectrometer to characterize the neutron spectrum (Machrafi et al., 2009).

3. Active detectors

Active dosimeters have many benefits in comparison to their passive counterparts. The ability to resolve dose rate over time allows for the separation of dose contribution from varying sources. For instance, spacecraft in low-Earth orbit are typically subject to galactic cosmic rays as a primary contributor of dose, but when traveling through the South Atlantic Anomaly they are subject to a high flux of trapped protons caused by an altitude dip in the Earth's magnetosphere. Active detectors have the added benefit of delivering dosimetry data in real time, which can reduce dose by alerting crew to the occurrence of a solar particle event.

Active detectors, however, are generally larger and require electricity which is in short supply onboard spacecraft. Modern improvements in microprocessors and battery capacity are helping to overcome these shortcomings, though a compact active personnel dosimeter has yet to be implemented for applications in space. Several types of active detectors have recently been used for characterization of the complex radiation environment (see Tables 2 and 3).

3.1. Silicon semiconductor

3.1.1. Liulin-4

The Liulin series of silicon detectors has been in operation since 1988 when its first incarnation was used on board the Mir space station. The Liulin-4 detector is not the latest model in this series, but the simple and compact design provides useful data in certain applications. This spectrometer contains a single silicon detector, charge-sensitive preamplifier, microcontrollers, and flash memory. The lithium-drifted silicon detector is 0.3 mm thick with an area of 2.0 cm^2. A 12 bit analog-to-digital converter is installed, though only 8 bits are used to provide 256 channels for energy spectrum construction over a time scale that is

Table 2
Comparison of active detectors.

Dosimeter	Type	Range of response	Determines (for particle[a])	Abs. vs. eq. dose	Portability
Liulin-4	Si semicond.	Charged particle flux: 0.01–1000 cm^{-2} s	Dose (Lo); flux (Hi)	Absorbed dose	Portable/battery power
DOSTEL	Si telescope	0.1–240 keV μm^{-1} (H_2O)	Dose, dose rate, LET (Lo, Hi)	Equivalent dose	Relocatable
RRMD-III	Si telescope	0.1–600 keV μm^{-1} (tissue)	Dose, dose rate, LET (Lo, Hi, N)	Equivalent dose	Relocatable
Liulin-5	Si telescope	0.07–110 keV μm^{-1} (H_2O)	Dose, dose rate, LET (Lo, Hi)	Equivalent dose	Relocatable
Liulin Phobos	Si telescope	0.75–155 keV μm^{-1} (H_2O)	Dose, dose rate, LET (Lo, Hi)	Equivalent dose	N/A
CPDS	Si telescope/ Cerenkov	0.1–20 keV μm^{-1} (H_2O)[b]	Dose, dose rate, LET (Lo, Hi)	Equivalent dose	Relocatable
TEPC	Prop. counter	0.2–600 keV μm^{-1} (tissue)[b]	Dose, dose rate, LET (Lo, Hi)	Equivalent dose	Relocatable
R-16	Ion chamber	0.4–1000 mrad h^{-1}	Dose, dose rate (Lo, Hi)	Absorbed dose	Stationary
BBND	^{3}He prop. counters	Neutrons: thermal – 15 MeV	Dose, dose rate (N)	Equivalent dose	Stationary

[a] Hi = high-LET charged particle; Lo = low LET (electron, gamma); N = neutron.
[b] Estimated from calibration data.

Table 3
Notes and references.

Dosimeter	Notes	Sources
Passive		
Plastic nuclear track detector	Best passive method for high-LET; used in conjunction with luminescent detectors and foils	Zhou et al. (2008), Benton et al. (2001b)
Luminescent detector	TLD: some high-LET data can be obtained from HTR techniques; OSLD: newer technology, more capability	Vana; Bilski; Berger; Horowitz
Photographic emulsion	Adjustable sensitivity; requires film development; not commonly used	Akopova et al. (2005)
Metal foil	Activation method: inaccurate in low-flux fields; fission method: fragments detected by NTD	Badhwar et al. (2002), Benton et al. (2001)
"Pille" TLD	Portable readout; no LET determination	Apáthy et al. (2002, 2007)
MOSFET	Portable readout; no LET determination	Thomson and Nielsen (1999), Kohno et al. (2006)
Bubble detector	Portable readout; used for N detection; heavy charged particles convolute results slightly	Machrafi et al. (2009), Ing (2001)
Active		
Liulin-4	Cannot determine LET; pocket-sized for mobile monitoring	Dachev et al. (2002)
DOSTEL	Assumes mean-chord-length across FOV in LET calculation	Beaujean et al. (2002)
RRMD-III	Determines path length with PSDs	Doke et al. (2001, 2004)
Liulin-5	Assumes mean-chord-length across FOV in LET calculation	Semkova et al. (2004, 2007)
Liulin Phobos	Assumes mean-chord-length; orthogonal telescopes	Dachev et al. (2009)
CPDS	Determines path length with PSDs; can determine species for C, N, and O particles	Lee et al. (2007)
TEPC	Assumes mean-chord-length for all angles; LET assumed equal to y (Lineal energy)	Badhwar et al. (1996), Gersey et al. (2002, 2007)
R-16	Pulse-type ion chamber: 1 pulse per 5 mrad; shallow and deep dose rates; assumes average LET	Mitricas et al. (2002), Badhwar (2000)
BBND	Heavy system; short-term experiment; requires ^{3}He	Koshiishi et al. (2007), Matsumoto et al. (2001)

selectable between 10 and 3539 s, in 10 s intervals. The pulse height is determined after the preamplifier and divided among the 256 energy channels, ranging from 0.02 MeV to 20 MeV. Energy depositions greater than 20 MeV are recorded in the highest-energy channel.

To determine dose in this detector type, the energy deposition in each channel is determined by multiplying the number of counts in the channel by the channel's energy. Those results are divided by the mass of the detector volume and summed to determine a total dose across all channels. The recorded energy distribution shape may provide additional useful information regarding the nature of the dominant radiation field (SAA, GCR, etc.), but does not provide enough detail to determine an effective LET of the incident radiation.

The size and portability of the Liulin-4 type spectrometer makes it a viable candidate for active personnel dosimetry in the event of a solar particle event, but limitations in the ability to determine effective LET and equivalent dose likely prevent this detector design from usurping the importance of the passive detection methods mentioned above (see Section 2). The Liulin-4 comes in many variations with options that can run on either battery or continuous power, operate with or without an external display, and can even incorporate a GPS receiver (Dachev et al., 2002). The flexibility and continuous improvement upon this design, along with a fairly simple detection system, make for an effective device, but one which suffers from limited functionality.

3.2. Silicon telescope

3.2.1. DOSTEL

The DOSimetry TELescope was developed in 1995 as a small particle telescope for use on space shuttle missions to the Mir space station. The design incorporated two PIPS silicon detectors arranged as a telescope (see Fig. 2). Each detector is 0.315 mm thick with a 6.93 cm^2 sensitive area. A gap of 15 mm between the detectors provides a geometric factor of 824 mm^2 sr (a unit of measure determined by the detector's active area and field of view) for detection of coincidence events. Each detector connects to a charge sensitive amplifier, 2 pF integrating capacitor, two-step pulse amplifier, two peak detectors, two RC-filters for noise reduction, and an 8-bit ADC. This arrangement

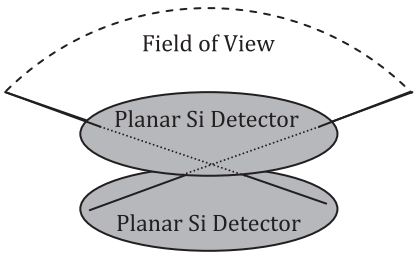

Fig. 2. Cross-section diagram of DOSTEL detector arrangement. Adapted from Beaujean et al. (2002).

allows for pulse height analysis across separate low energy and high energy ranges.

When a coincident event is recorded in both detectors, it is possible to determine the LET of the incident radiation. Because the trajectory of the particle is known to be within a limited cone of possible directions, an average thickness of the detector can be used to estimate the track length of energy deposition. By dividing the deposited energy over this mean path-length (0.364 mm) with a density of 2.33 g cm^{-3}, an approximation of linear energy transfer is possible. The result must be multiplied by a coefficient to account for the difference of LET in silicon versus LET in water. In this manner, the DOSTEL instrument can record LET (in water) from 0.1 to 240 keV μm^{-1} (Beaujean et al., 2002).

This instrument features a relatively simple design and can reliably determine equivalent dose and dose rate, though its assumption of mean chord-length diminishes accuracy in LET determination compared to instruments that utilize position sensitive detectors (see Sections 3.2.2 and 3.2.5). The directional nature of the device allows determination of dose contributions by trapped protons in the Earth's radiation belts versus galactic cosmic rays and solar particle events (Reitz, 2006).

3.2.2. RRMD III

The Real-time Radiation Monitoring Device (RRMD-III) was developed in the mid-1990s for the Japanese space program NASDA in collaboration with Waseda University (Doke et al., 2001). The design sought to improve accuracy of LET determination by including a measurement of particle incident angle in its calculation of LET. To accomplish this, three double-sided silicon strip detectors (DSSD) are stacked with a gap of 4.5 mm between them (see Fig. 3). Each DSSD has an active area of 20 mm × 20 mm with a thickness of 0.5 mm. Sixteen detector strips are positioned on each side, oriented orthogonally to those on the opposite side, allowing for an X–Y coordinate of interaction to be determined within each DSSD. In a coincidence event between the DSSDs, the angle of incidence can be determined by comparing the locations of interaction within each detector. The middle DSSD is then used as a standard detector for determination of dose and LET by dividing the deposited energy over the effective thickness of material traversed. Rather than rely upon an assumption of mean path-length, such as described for the DOSTEL instrument, the measured angle of incidence accounts for any off-axis deviation from the normal path-length.

Thanks to a symmetrical detector layout, the instrument is capable of detecting particles entering from either the front or back. Detector windows on each side are covered by two aluminum foil sheets with thicknesses of 0.1 mm and 0.4 mm. A later improvement upon the design incorporates a 10 mm thick slab of acrylic to aid in the measurement of fast neutrons. The system is capable of measuring incident LET from 0.1 keV μm^{-1} to 600 keV μm^{-1} (Doke et al., 2001, 2004), allowing for determination of equivalent dose and dose rate.

3.2.3. Liulin-5

The Liulin-5 detector was designed as an improvement upon the original Liulin series in coordination with the MATROSHKA-R experiment, which sought to determine depth-dose within a spherical tissue equivalent phantom (Semkova et al., 2004). This unit may share some components with the Liulin-4, but otherwise bears little resemblance. The system utilizes three PIN photodiode silicon detectors in a cylindrical aluminum tube arranged as a telescope (see Fig. 4). The tube slips into the phantom with the innermost tip of the detector resting at the center of the sphere. The two outer detectors (D1 and D2), with their active surfaces pointed outward, are designed to operate in coincidence for the determination of LET. The innermost detector (D3) points its active surface into the center of the phantom and is primarily used for determination of dose to deep organs, though it can also operate in coincidence with D1 to provide additional LET data. Each

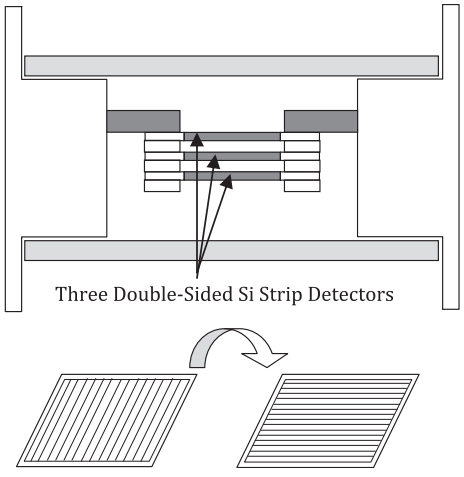

Fig. 3. Cross-section diagram of RRMD-III unit and double-sided strip detector. Adapted from Doke et al. (2001, 2004).

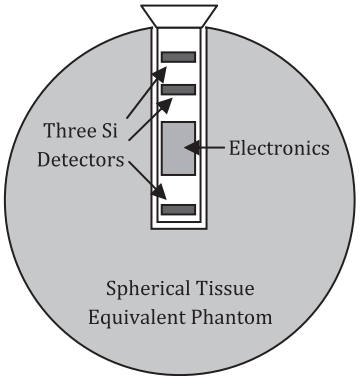

Fig. 4. Cross-section diagram of Liulin-5 detector within MATROSHKA-R spherical phantom. Adapted from Semkova et al. (2007).

detector is 0.4 mm thick, with an active layer of approximately 0.3 mm. The area of each detector is not consistently described in the available literature, but is approximately 2 cm^2.

By using multiple detectors in coincidence, the Liulin-5 can provide a wealth of data regarding the energy deposition spectrum, as well as incident LET. If a particle traverses both D1 and D2 within a 98° cone of sensitivity, the data can be used to determine incident LET and dose. In the event of coincidence detection in D1 and D3 (which has a much smaller cone of sensitivity due to the increased distance between detectors), the LET can be determined as well. The D3 detector operates with a different gain, however, which allows determination of LET across a broader range.

The Liulin-5 instrument provides data for dose rates between 40 nGy h^{-1} and 40 mGy h^{-1}, flux between 0 and 400 cm^{-2} s^{-1}, energy deposition across 0.3–80 MeV in the outer detectors, and 0.05–10 MeV in the inner detector (Semkova et al., 2004, 2007). Characterization of the LET environment permits the calculation of equivalent dose and dose rate, while inclusion within the tissue equivalent phantom provides a measurement of deep dose.

3.2.4. Liulin Phobos

An extension of the techniques developed for the Liulin-5 dosimeter on the International Space Station, the Liulin Phobos instrument will be used to assess the dose rate on a descent module to Mars' moon Phobos (Dachev et al., 2009). This unit is comprised of four detectors in a square arrangement to function as two perpendicular telescopes. Each detector operates in coincidence with the opposing detector to determine an effective LET for each event, using the techniques mentioned under the description of DOSTEL (see Section 3.2.1). Much like DOSTEL, the Liulin Phobos is also capable of isolating solar particle events from galactic cosmic rays due to its directional telescope design.

Many components are carried over from the Liulin-5 instrument. Four silicon PIN photodiode detectors, each with an active thickness of 0.3 mm, connect to four charge sensitive preamplifiers. A microprocessor, flash memory, and other circuitry are included within the rectangular case. Dose rate can be measured from 40 nGy h^{-1} to 100 mGy h^{-1}. Each of the two telescopes can detect energy depositions from 0.1 MeV to 90 MeV and discriminate LET (in water) from 0.75 keV μm^{-1} to 155 keV μm^{-1} (Dachev et al., 2009), allowing determination of equivalent dose and dose rate.

3.2.5. Charged particle directional spectrometer (CPDS)

The charged particle directional spectrometer was first used onboard the International Space Station in 2002 (Lee et al., 2007). The CPDS provides a wealth of data to characterize the radiation environment. One CPDS, deemed IV-CPDS, is located within the US Lab Module. Three others are mounted on a boom outside of the spacecraft in three directions, collectively known as the EV-CPDS. One of these external units has failed, however, so only two detectors continue to operate.

Each detector consists of a stack of 12 silicon detectors situated above a sapphire Cerenkov detector and photomultiplier tube (PMT) (see Fig. 5). Three types of silicon detectors are used within the silicon detector stack. Three, 1 mm thick square detectors with 30 mm sides are used as trigger detectors for coincidence events. Three position sensitive detectors with 0.30 mm thickness and 24 mm square sides are used to determine incidence angle. Each position sensitive detector consists of 24 silicon strip detectors on top and 24 orthogonal silicon strip detectors on bottom to provide an X–Y position of interaction within the unit. Six cylindrical lithium drifted silicon detectors are positioned on either side of three cards and are used for LET determination and spectroscopy. Each has a thickness of 5 mm and an active diameter of 58.4 mm. The Cerenkov detector utilizes a 10 mm thick, 50 mm diameter sapphire crystal to produce Cerenkov light from high energy particles.

One coincidence signal detector is situated in front of two position sensitive detectors near the aperture of the instrument, followed by another coincidence signal detector. Below this, the six lithium drifted detectors are closely

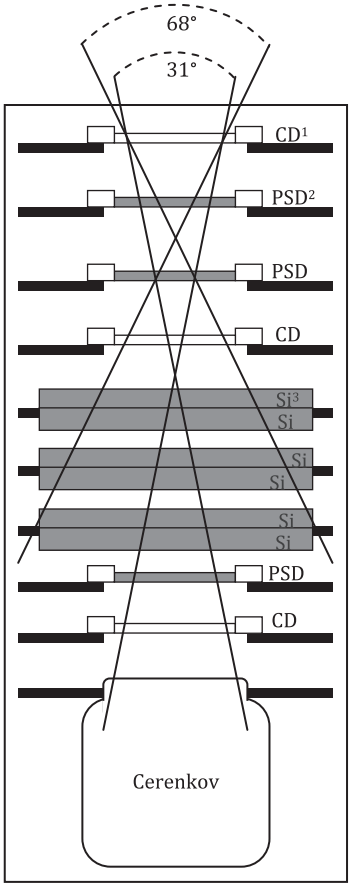

Fig. 5. Cross-section diagram of CPDS). (1) Coincidence detector; (2) position sensitive detector; (3) Li-drifted silicon detector. Adapted from Lee et al. (2007).

stacked. These 10 detectors are capable of detecting particles within a 68° field of view. Below this, the third position sensitive detector sits above the third coincidence signal and Cerenkov detector. Due to the increased distance from the aperture, the Cerenkov system detects particles within a narrower 31° field of view, but across a higher energy range.

Because of the multitude of detectors and the Cerenkov unit, the CPDS is capable of producing detailed energy spectra up to 400 MeV/nucleon. Particle charge can be determined for particles up to $Z = 12$ and energy spectra can be generated for particles with $Z < 4$ (Lee et al., 2007). These systems produce an exorbitant amount of data, however, which requires extensive processing to provide relevant information. Much like the RRMD-III (see Section 3.2.2), the CPDS can determine angle of incidence for particles, allowing an accurate assessment of LET and equivalent dose.

3.3. Gas filled detectors

3.3.1. Tissue equivalent proportional chamber (TEPC)

The tissue equivalent proportional chamber (TEPC) was developed as an active dosimeter to replace the original Rossi counter (Doke et al., 2001). A volume of gas within a sealed chamber is subject to an applied voltage. As ionization occurs within the detection volume, electrons liberated from their positive-ion counterparts are free to drift within the chamber. The electric field causes electrons to accelerate toward the anode wire, colliding with other gas molecules and generating additional ion pairs. This gas multiplication phenomenon improves the proportional counter's ability to determine dose in radiation fields with lower flux as compared to an ion chamber, lending itself to applications in space where flux is comparatively low (Knoll, 2000).

The TEPC developed for NASA is a cylinder of 5 cm diameter and 5 cm length, with its shell constructed of A150 tissue equivalent plastic. The chamber is filled with propane at very low pressure to simulate a tissue cylinder of 2 μm diameter. In its application for dosimetry in space, energy deposition can be determined through pulse height analysis. By dividing absorbed dose over the mean-chord-length, lineal energy can be estimated. Under the assumption that mean lineal energy is equal to LET, the system is then able to calculate an equivalent dose and dose rate in real time (Badhwar et al., 1996). These assumptions have since been shown to be inaccurate with an error of up to twenty percent when characterizing response from a controlled HZE beam in an accelerator (Gersey et al., 2002), though continuing research by many groups work to improve the accuracy of response to HZE particles (Gersey et al., 2007). Regardless, the TEPC continues to provide reliable data for radiation monitoring and connects into an automatic alarm system to alert the crew in the event of a radiation storm.

3.3.2. R-16 ion chamber

The R-16 dosimeter was the primary radiation monitoring instrument onboard the Mir space station and is still used onboard the Russian segment of the International Space Station (Badhwar, 2000). The instrument incorporates two separate ion chambers with different shielding thicknesses for measurements of both skin dose and dose to blood-forming organs.

Each chamber is shaped as a 60 mm diameter cylinder with hemispherical ends and filled with argon to a pressure of up to 4.5×10^5 Pa. Both are shielded by 0.5 g cm^{-2} of aluminum while one chamber is shielded by an additional 3.0 g cm^{-2} of tissue equivalent glass (Mitricas et al., 2002). The instrument operates in pulse mode using an electrostatic relay to build up a charge that equates to a dose of 50 μSv before signaling a pulse. Though the system is arguably outdated, the simplistic output from this detection system does benefit by minimizing bandwidth for transmission between spacecraft and Earth, with a number of pulses equating to an accumulated dose.

The R-16 is capable of measuring absorbed dose rate for shallow and deep tissues from 0.4 to 1000 mrad h^{-1} with an accuracy of ±20–30%, but is incapable of determining LET data (Badhwar, 2000). Effective dose is therefore determined during calibration using average quality factors obtained by other means.

3.4. Neutron detector

3.4.1. Bonner ball neutron detector

A major deficiency in space dosimetry has been the detection of neutrons, which have been estimated to contribute 30–60% of the total equivalent dose in space (Benton and Benton, 2001). The Bonner Ball Neutron Detector was used onboard the ISS from 23 March to 14 November 2001, in an experiment to evaluate the neutron radiation environment. The instrument contains six spherical ^{3}He proportional counters of two inch diameter, encased in moderators of two types with varying thickness. Four detectors were moderated by polyethylene spheres of 1.5, 3, 5, and 9 cm thickness. Gadolinium covers of 1 mm thickness were added to the detector using 1.5 cm of polyethylene, as well as an unmoderated detector, to eliminate thermal neutrons. The remaining detector had no shielding or moderator. All six sensors were encased in a single large detector unit (Koshiishi et al., 2007).

Each detector was calibrated to form thermal neutron peaks in specific output channels so as to discriminate neutrons from charged particles. The BBND can therefore measure neutron fields from thermal to 15 MeV with an accuracy of approximately 15% (Matsumoto et al., 2001). While the equivalent dose from neutrons can be obtained from the acquired data, it should be noted that the BBND was a temporary experiment rather than a dosimeter for continuous operation.

4. Conclusion

The estimation of dose from radiation in space poses many challenges. In spite of restraints to cost, size, weight, and power consumption, detectors must provide information beyond what is often required in terrestrial applications. In addition to resolving dose and dose rate in an environment with relatively low flux, dosimeters should be capable of determining the ionization density of incident particles. Passive dosimetry methods continue to provide the most relevant data, but often require extensive processing after returning to Earth. Active detectors can provide time-resolved data in real time, but size and power consumption prevent these instruments from operating as personnel dosimeters. Neutron dosimetry provides an additional challenge that must be met to accurately estimate the effective dose to astronauts.

Sights have been set upon Mars as the next great leap of human achievement, but one of the practical challenges to accomplishing this goal is the accurate assessment of radiation dose received by astronauts during such an extended voyage. As technology continues to decrease in both size and cost, it is imperative that research and development focus upon utilizing such advancements to provide a dosimetry system capable accurately resolving equivalent dose and dose rate in a compact and convenient manner.

References

Akopova, A.B., Manaseryan, M.M., Mekonyan, A.A., et al. Radiation measurement on the International Space Station. Radiation Measurements 39, 225–228, 2005.

Apáthy, I., Deme, S., Fehér, I., et al. Dose measurements in space by the Hungarian Pille TLD system. Radiation Measurements 35, 381–391, 2002.

Apáthy, I., Akatov, Yu.A., Arkhangelsky, V.V., et al. TL dose measurements on board the Russian segment of the ISS by the "Pille" system during Expedition-8, -9 and -10. Acta Astronautica 60, 322–328, 2007.

Badhwar, G.D., Golightly, M.J., Konradi, A., et al. In-flight radiation measurements on STS-60. Radiation Measurements 26 (1), 17–34, 1996.

Badhwar, G.D. Radiation measurements on the International Space Station, in: 1st International Workshop on Space Radiation Research and 11th Annual NASA Space Radiation Health Investigators' Workshop, Arona (Italy), May 27–31, 2000.

Badhwar, G.D., Atwell, W., Reitz, G., et al. Radiation measurements on the Mir Orbital Station. Radiation Measurements 35, 393–422, 2002.

Ballarini, F., Battistoni, G., Cerutti, F., et al. GCR and SPE organ doses in deep space with different shielding: Monte Carlo simulations based on the FLUKA code coupled to anthropomorphic phantoms. Advances in Space Research 37, 1791–1797, 2006.

Beaujean, R., Kopp, J., Burmeister, S., et al. Dosimetry inside MIR station using a silicon detector telescope (DOSTEL). Radiation Measurements 35, 433–438, 2002.

Benton, E.R., Benton, E.V. Space radiation dosimetry in low-earth orbit and beyond. Nuclear Instruments and Methods in Physics Research B IS4 (1–2), 255–294, 2001.

Benton, E.R., Benton, E.V., Frank, A.L. Neutron dosimetry in low-earth orbit using passive detectors. Radiation Measurements 33, 255–263, 2001.

Berger, T., Hajek, M., Fugger, M., et al. Efficiency corrected dose verification with thermoluminecence dosemeters in heavy ion beams. Radiation Protection Dosimetry 120, 361–364, 2006.

Berger, T., Hajek, M., Summerer, L., et al. Austrian dose measurements onboard space station MIR and the International Space Station – overview and comparison. Advances in Space Research 34, 1414–1419, 2004.

Bilski, P. On the correctness of the thermoluminescent high-temperature ratio (HTR) method for estimating ionization density effects in mixed radiation fields. Radiation Measurements 45, 42–50, 2010.

Bilski, P. Dosimetry of densely ionising radiation with three LiF phosphors for space applications. Radiation Protection Dosimetry 120, 397–400, 2006.

Dachev, Ts., Tomov, B., Matviichuk, Yu., et al. Calibration results obtained with Liulin-4 type dosimeters. Advances in Space Research 30 (4), 917–925, 2002.

Dachev, Ts., Semkova, J., Maltchev, S., et al. Radiation environment study during Phobos sample return mission by charged particle telescope Liulin-Phobos, in: 40th Lunar and Planetary Science Conference, 2009.

Doke, T., Hayashi, T., Kikuchi, J., et al. Measurements of LET-distribution, dose equivalent and quality factor with the RRMD-III on the Space Shuttle Missions STS-84, -89 and -91. Radiation Measurements 33, 373–387, 2001.

Doke, T., Fuse, T., Hara, K., et al. Measurement of linear energy transfer distribution at CERN-EU high-energy reference field facility with real-time radiation monitoring device III and its comparison with dosimetric telescope. Japanese Journal of Applied Physics 43 (6A), 3576–3581, 2004.

Gersey, B.B., Borak, T.B., Guetersloh, S.B., et al. The response of a spherical tissue-equivalent proportional counter to iron particles from 200–1000 MeV/nucleon. Radiation Research 157, 350–360, 2002.

Gersey, B.B., Aghara, S., Wikins, R., et al. Comparison of a tissue equivalent and a silicon equivalent proportional counter microdosimeter to high-energy proton and neutron fields. IEEE Transactions on Nuclear Science 54, 2276–2281, 2007.

Halill, A., Brown, M., Akatov, Yu., et al. MOSFET dosimetry mission inside the ISS as part of the MATROSHKA-R experiment. Radiation Protection Dosimetry 138 (4), 295–309, 2010.

Horowitz, Y.S., Satinger, D., Fuks, E., et al. On the use of LiF:Mg,Ti thermoluminescence dosemeters in space – a critical review. Radiation Protection Dosimetry 106 (1), 7–24, 2003.

Ing, H. Neutron measurements using bubble detectors – terrestrial and space. Radiation Measurements 33, 275–286, 2001.

Knoll, G. Radiation Detection and Measurement. John Wiley & Sons, Ann Arbor, 2000.

Kohno, R., Nishio, T., Miyagishi, T., et al. Experimental evaluation of a MOSFET dosimeter for proton dose measurements. Physics in Medicine and Biology 51, 6077–6086, 2006.

Koshiishi, H., Matsumoto, H., Chishiki, A., et al. Evaluation of the neutron radiation environment inside the International Space Station based on the Bonner Ball Neutron Detector experiment. Radiation Measurements 42, 1510–1520, 2007.

Lee, K., Flanders, Joel, Semones, E., et al. Simultaneous observation of the radiation environment inside and outside the ISS. Advances in Space Research 40, 1558–1561, 2007.

Machrafi, R., Garrow, K., Ing, H., et al. Neutron dose study with bubble detectors aboard the International Space Station as part of the MATROSHKA-R experiment. Radiation Protection Dosimetry 133 (4), 200–207, 2009.

Matsumoto, H., Goka, T., Koga, K., et al. Real-time measurement of low-energy-range neutron spectra on board the space shuttle STS-89 (S/MM-8). Radiation Measurements 33, 321–333, 2001.

Mitricas, V.G., Tsetlin, V.V., Teltsov, M.V., et al. Radiation dose measurements aboard the Mir using the R-16 instrument. Radiation Measurements 35, 515–525, 2002.

Reitz, G. Past and future application of solid-state detectors in manned spaceflight. Radiation Protection Dosimetry 120, 387–396, 2006.

Semkova, J., Koleva, R., Todorova, G., et al. Instrumentation for investigation of the depth-dose distribution by the Liulin-5 instrument of a human phantom on the Russian segment of ISS for estimation of

the radiation risk during long term space flights. Advances in Space Research 34 (6), 1297–1301, 2004.

Semkova, J., Koleva, R., Shurshakov, V., et al. Status and calibration results of Liulin-5 charged particle telescope designed for radiation measurements in a human phantom onboard the International Space Station. Advances in Space Research 40, 1586–1592, 2007.

Simonsen, L.C., Wilson, J.W., Kim, M.H., et al. Radiation exposure for human Mars exploration. Health Physics 79 (5), 515–525, 2000.

Thomson, I., Nielsen, E. EVA dosimetry in manned spacecraft. Mutation Research 430, 203–209, 1999.

Vana, N., Schöner, W., Fugger, M., et al. Absorbed dose measurement and LET determination with TLDs in space. Radiation Protection Dosimetry 66 (1–4), 145–152, 1996.

Yukihara, E.G., Sawakuchi, G.O., Guduru, S., et al. Application of the optically stimulated luminescence (OSL) technique in space dosimetry. Radiation Measurements 41, 1126–1135, 2006.

Zhou, D., O'Sullivan, D., Semones, E., et al. Radiation dosimetry for high LET particles in low Earth orbit. Acta Astranautica 63, 855–864, 2008.